Manganese Stearate Initiated Photo-Oxidative and Thermo-Oxidative Degradation of LDPE, LLDPE and Their Blends

Prasun Kumar Roy,[1] Priyanka Singh,[2] Devendra Kumar,[2] Chitra Rajagopal[1]

[1]*Centre for Fire Explosive and Environment Safety, Research and Development Organization, Delhi 110054, India*
[2]*Delhi College of Engineering, Department of Applied Chemistry and Polymer Technology, Delhi 110042, India*

Received 22 November 2008; accepted 6 May 2009
DOI 10.1002/app.31252
Published online 22 March 2010 in Wiley InterScience (www.interscience.wiley.com).

ABSTRACT: This study is an attempt to investigate the effect of a representative pro-oxidant (manganese stearate) on the degradation behavior of 70 ± 5 μ thickness films of LDPE, LLDPE and their blends. Films were prepared by film blowing technique in the presence of varying quantities of manganese stearate (0.5–1% w/w) and subsequently subjected to accelerated degradative tests: xenon arc exposure and air-oven exposure (at 70°C). The physico–chemical changes induced as a result of aging were followed by monitoring the mechanical properties (Tensile strength and Elongation at break), carbonyl index (CI), morphology (SEM), melt flow index (MFI), oxygen content (Elemental analysis), and DSC crystallinity. The results indicate that the degradative effect of pro-oxidant is more pronounced in LDPE than LLDPE and blends, due to the presence of larger number of weak branches in the former. The degradation was also found to be proportional to the concentration of the pro-oxidant. Flynn-Wall-Ozawa iso-conversion technique was used to determine the kinetic parameters of degradation, which were used to determine the effect of the pro-oxidant on the theoretical lifetime of the polymer. J Appl Polym Sci 117: 524–533, 2010

Key words: ageing; degradation; polyethylene; pro-oxidant; photo-oxidation; thermo-oxidation

INTRODUCTION

Packaging polymers, particularly polyethylene films, have been considered to be the major culprit for causing the rising environmental pollution problem. These polymers, after completing their useful short lifecycle as packaging films, find their way to constitute the major fraction of solid municipal waste, where they refuse to degrade because of their hydrophobic nature. The problem aggravates due to the high molecular weight associated with these polymers. An acceptable solution to this problem is the use of oxo-degradable polyethylene, which first disintegrates to small pieces, thereby reducing their ubiquitous visual presence. In the process, their molecular weight is reduced and these become potentially biodegradable organics, which can be subsequently consumed by the microorganism to form biomass.[1–3] Major strategies to facilitate the disintegration and subsequent biodegradation of polyethylene are mainly focused on the direct incorporation of carbonyl groups within the backbone of the polymer (ethylene —CO copolymer)[4] or by addition of certain pro-oxidants (Scott-Gilead Process) during the processing stage.[5,6] These pro-oxidants, in the presence of either light or heat lead to the generation of free radicals on the polymer chain, which further react with oxygen to form carbonyl groups through a series of reactions. These carbonyl groups, then undergo photochemical reactions (Norrish Type I, II, and III) to finally lead to chain scission and physical embrittlement.[4]

In the recent years, linear low density polyethylene (LLDPE) is fast replacing low density polyethylene (LDPE) as packaging films, because of its better mechanical properties and comparable cost. Keeping in mind the increased use of LLDPE, we felt the need of performing accelerated degradation studies on LDPE, LLDPE, and LLDPE –LDPE blends. As a part of our ongoing efforts towards development of oxo-degradable polyethylene, we have reported the pro-oxidative action of cobalt stearate on LDPE,[7,8] which first leads to the abiotic disintegration of the matrix. The degradation of these disintegrated films by bacterial consortium has also been reported.[9] The effect of such pro-oxidants is expected to be less pronounced for LLDPE because of the lesser degree of branching in the polymer chain, therefore requiring higher concentrations of the pro-oxidant to reach the same level of degradation, which has been confirmed by our investigations.[10] To avoid the slight bluish tinge in the films containing higher concentrations of cobalt stearate,

Correspondence to: P. K. Roy (pk_roy2000@yahoo.com).

the present investigation was performed on films containing manganese stearate which also belong to the broad category of pro-oxidants.[11]

EXPERIMENTAL

Materials

Manganese chloride, sodium hydroxide, stearic acid, ("AR" grade E.Merck) were used without further purification. Commercial linear low density polyethylene (LLDPE GleneF20S009) and General purpose film grade low density polyethylene (LDPE 24FS040) have been used to prepare films. The melt flow index (MFI) of LLDPE and LDPE was determined to be 0.9 g/10 min and 3.6 g/10 min respectively. Manganese stearate was prepared by double decomposition reaction of manganese chloride with sodium stearate according to the procedure reported in the literature.[12] Milli Q ultrapure water was used throughout the course of this work.

Characterization of pro-oxidant

The structural characterization of manganese stearate was performed by FTIR spectroscopy (BIORAD FTS-040). The thermal analysis i.e. thermogravimetry (TG) and Differential scanning calorimetric analysis (DSC) was performed using a Perkin–Elmer Diamond Simultaneous TGA-DTA-DSC instrument under nitrogen atmosphere in the temperature range 30–500°C at a constant heating rate of 10°C min^{-1}. The C, H, and O content in the pro-oxidant was determined by an elemental analyser (Elementar, Vario EL) and the metal content was determined by first digesting the sample in HCl to bring the metal to aqueous phase, which was then subsequently analyzed by Perkin–Elmer Inductively Coupled Plasma spectrophotometer (Optima2000). The fatty acid content, nonvolatile content and ash content were determined as per the procedure reported in the literature.[13]

Film preparation

Films of 70 ± 5 μ thickness were prepared by mixing varying concentrations of manganese stearate (0.5–1% w/w) in an extruder attached to a film blowing unit. The temperature in the barrel sections of the extruder was maintained at 120°C and 130°C respectively, and that of the die head section was maintained at 140°C.

The sample codes of all the composition prepared along with their MFI are reported in Table I. The blow up ratio (B.U.R) and draw down ratio (D.D.R) values were calculated according to the following formula. B.U.R = d/D, D.D.R = H/H_0, where d is the diameter of the bubble, D is the diameter of the die, H is the die gap and H_0 is the thickness of the films.

TABLE I
Sample Designation and their Formulations

Sample designation	Amount (g) LDPE	LLDPE	Manganese stearate	MFI (g/10 min)
LMS0	300	–	–	3.6
LMS50	300	–	1.5	3.6
LMS75	300	–	2.25	3.7
LMS100	300	–	3	3.7
LLMS0	–	300	–	0.9
LLMS75	–	300	2.25	0.9
L25MS0	75	225	–	1.4
L25MS75	75	225	2.25	1.4
L50MS0	150	150	–	2
L50MS75	150	150	2.25	2
L75MS0	225	75	–	2.8
L75MS75	225	75	2.25	2.8

Both B.U.R and D.D.R give a measure of the extensibility of the material towards transverse and machine direction respectively. Our studies indicate that manganese stearate did not affect the extensibility of the polymer and all films were prepared by maintaining a B.U.R of 5.5:1 and a D.D.R of 14.2.

Degradation studies

Photodegradation studies

Accelerated photodegradation studies were carried out using a Xenon arc apparatus set at 550 Wm^{-2} as per ISO 4892-2:1994. The Black panel temperature was set at 63°C for the entire exposure period.

Thermo-oxidative tests

The thermo-oxidative testing was carried out by placing the blown films in an air oven at 70°C ± 1, which corresponds to the maximum temperature achieved during composting conditions.[14]

Monitoring of degradation: Analytical characterization

Mechanical properties

The tensile tests were performed on test specimens according to ASTM 882-85 using a Materials testing machine (Model JRI-TT25). Films (5 cm × 1 cm) were subjected to a crosshead speed of 50 cm min^{-1}. The tests were undertaken at 25°C and a relative humidity of 65%. Five samples were tested for each experiment and the average value has been reported.

Spectroscopic investigations

The structural changes in the film was investigated using FTIR spectroscopy. Carbonyl index (CI), was used as a parameter to monitor the degree of photo-oxidation of polyethylene, and has been calculated according to the baseline method.[15]

$$\text{Carbonyl index (CI)} = \frac{\text{Absorption at 1740 cm}^{-1}\text{ (the maximum of carbonyl peak)}}{\text{Absorption at 1460 cm}^{-1}\text{ (internal thickness band)}}$$

Thermal properties

The thermal behavior was investigated in the temperature range 50–500°C at a constant heating rate of 10°C min^{-1}. The percentage crystallinity was calculated from the DSC traces as follows:

$$\%\ \text{Crystallinity} = \frac{(\Delta H_{f,\ observed})}{\Delta H_{f,\ (100\%\ \text{crystalline})}} \times 100$$

where ΔH_f is the enthalpy associated with melting of the material and $\Delta H_{f(100\%\ \text{crystalline})}$ is the enthalpy of 100% crystalline polyethylene reported in the literature to be 285 J/g.[16]

Melt flow index

The Melt Flow indices of samples was measured using an MFI instrument (International Equipments, Mumbai) at 190°C as per ASTM D1238. The extrudates were cut at regular intervals of 30s under a load of 2.16 kg.

Morphological studies

Scanning electron microscopy was performed to investigate the changes in the morphology of films. Sample surfaces were sputtered with gold using usual techniques and then analyzed under electron microscope Model LEO1455, Cambridge, UK applying a voltage of 10 kV. Photo-micrographs were taken at uniform magnification of 2000-fold.

Kinetic evaluations

The kinetics of degradation was evaluated by nonisothermal thermogravimetric analysis under flowing atmosphere of nitrogen at a purge rate of 200 mL/min. The sample was equilibrated to 200°C before being heated to 550°C at different heating rates (3–10°C/min). The actual heating rate was calculated from temperature measurements made during the period of polymer decomposition.

RESULTS AND DISCUSSION

Characterization of pro-oxidant

Manganese stearate was prepared by the double decomposition reaction of manganese chloride with sodium stearate and the resultant pink precipitate was filtered, dried and subsequently recrystallised in toluene. The stearate was found to be soluble in nonpolar solvents like benzene, toluene, DMSO and insoluble in water and acetone. The nonvolatile content and ash content was found to be 98% ± 1% and 10.5% ± 0.9% respectively. The free fatty acid content was negligible for all practical purposes indicating that all the acidic functionalities were consumed during the reaction. Elemental analysis was used to determine the molecular formula of manganese stearate, which was calculated to be $(C_{17}H_{35}COO)_2.Mn.2H_2O$. The FTIR spectra of the stearic acid exhibited characteristic >C=O and C—O absorption bands at 1714 cm^{-1} and 1409 cm^{-1} respectively. An additional band at 1560 cm^{-1} was observed in manganese stearate, which can be attributed to the asymmetric vibration stretching of the carboxylic group coordinated to the metal ion. DSC analysis revealed that manganese stearate exhibited a melting point of approximately 115−120°C. TGA indicated that manganese stearate does not degrade under the processing conditions as indicated by a single step degradation at higher temperatures.

Degradation mechanism

The mechanism of the transition metal catalyzed degradation of polyethylene has been described in the literature to proceed via formation of free radical intermediates.[17,18] The electron in the 3d subshell of manganese in $(C_{17}H_{35}COO)_2.Mn.2H_2O$ absorbs energy (as heat/light) and gets promoted to the higher level, which leads to the formation of $C_{17}H_{35}COO$. This decarboxylates to form $C_{17}H_{35}$, which abstracts hydrogen from the polyethylene chain, thereby initiating the degradation process.

Degradation studies

Mechanical properties

The variation in the longitudinal tensile strength (TS) and percent elongation at break (EAB) of polyethylene samples, both in the presence and absence of manganese stearate (0.75% w/w), as a function of air oven aging time is presented in Figures 1 and 2. It can be observed that TS and EAB were much higher for LLDPE (20.9 MPa and 93.8%) as compared to LDPE (9.6 MPa and 88.3%), and as expected, blending of LLDPE with LDPE led to intermediate properties. One important feature which can be noted from the figures, is the absence of processing degradation to the polymer, i.e., films containing manganese stearate exhibit initial mechanical

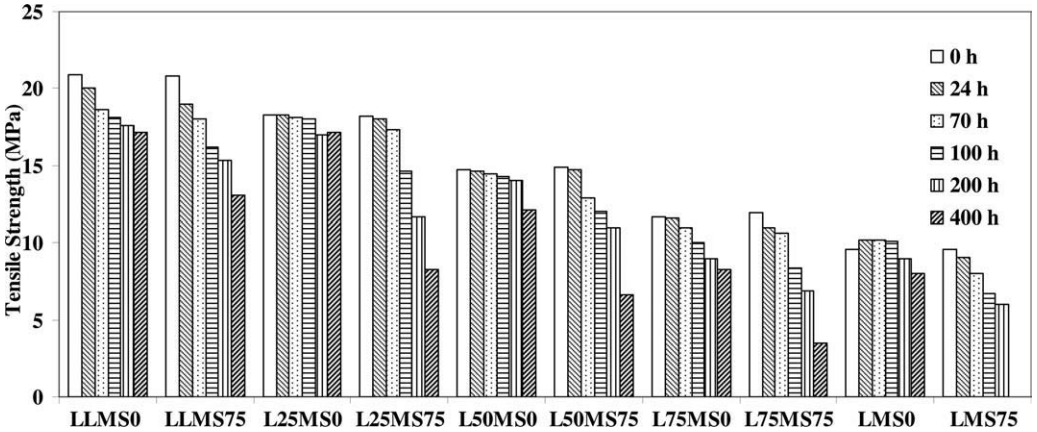

Figure 1 Decrease in tensile strength as a function of air oven aging.

properties in the same range as that of the neat film. However, the presence of manganese stearate led to a dramatic decrease in these properties when exposed to 70°C and the degradation was most pronounced in the case of LDPE.

The effect of xenon arc exposure on the mechanical properties of all the formulations are presented in Figures 3 and 4. On comparison, it can be seen that the degradation as a result of xenon arc exposure is more pronounced than thermo-oxidation. LDPE films containing pro-oxidant could not be tested after 75 h of xenon arc lamp exposure. Neat LLDPE samples retained their strength even after 400 h of exposure.

LDPE is relatively more susceptible to degradation because of the presence of large number of butyl branches (weak links), which are introduced during the ethylene high pressure polymerization process. On the other hand, LLDPE contain butene and hexene branches instead, at much lesser concentrations, and therefore offer lower number of tertiary weak sites for the oxidation to occur.

Structural properties

The change in the FTIR spectra of two representative samples (L75MS0 and L75MS75) as a result of both air oven aging and xenon arc exposure are presented in Figures 5 and 6. As can be seen, aging of neat films, i.e in the absence of pro-oxidant, do not lead to any appreciable changes in the FTIR spectra. However, aging of films containing trace quantities of pro-oxidant result in the formation of several functional groups, which absorb primarily in the carbonyl region ($\sim 1720\ cm^{-1}$), amorphous regions ($\sim 1300\ cm^{-1}$) and hydroxyl regions ($\sim 3300\ cm^{-1}$). The carbonyl band at $1720\ cm^{-1}$ is a result of the overlap of several absorption bands due to aldehyde and/or esters ($1733\ cm^{-1}$), carboxylic acid groups ($1700\ cm^{-1}$), and γ lactones ($1780\ cm^{-1}$),[19] all containing >C=O group in common. The degradation resulting from the aging process has been quantified by CI measurements. The change in the CI as a function of air oven exposure and xenon arc exposure has been presented in Figures 7 and 8 respectively. As is evident, there was negligible increase in the CI of neat films (i.e., films in the

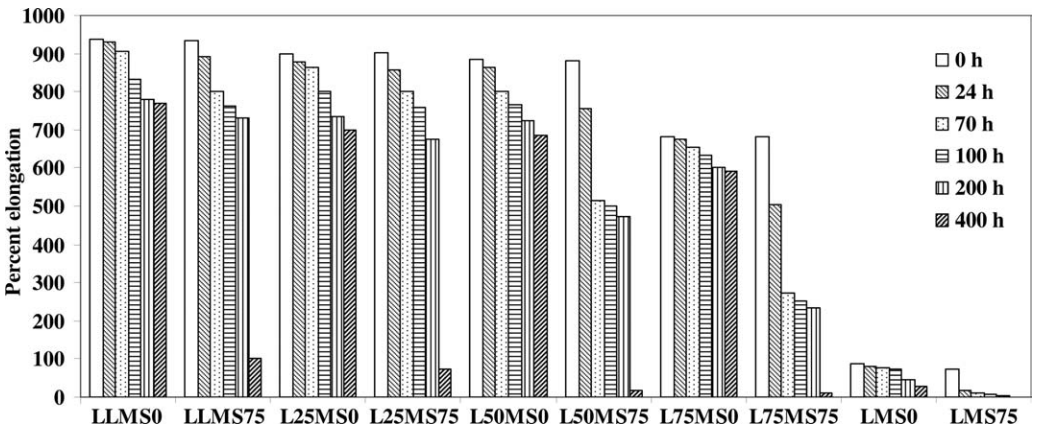

Figure 2 Decrease in percent elongation as a function of air oven aging.

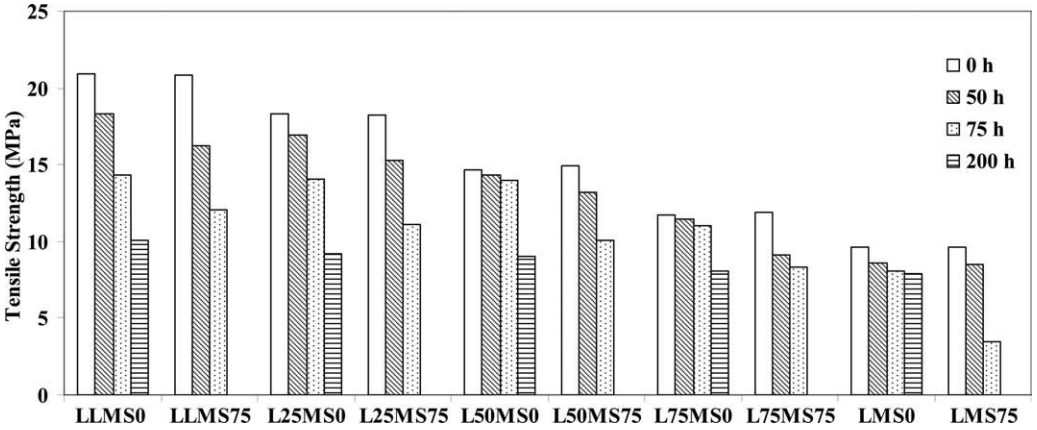

Figure 3 Variation in tensile strength as a function of xenon arc exposure.

absence of pro-oxidant), whereas a substantial increase was observed in the CI of films containing manganese stearate. It is generally believed that polyethylene films enter decay stage at CI greater than 6.[20] Films in the absence of pro-oxidant does not reach this stage during the period under investigation. The effect of manganese is more pronounced in LDPE and all these formulations reach decay stage within 60 h of air-oven exposure. LDPE films containing pro-oxidant could not be tested after 75 h of xenon arc lamp exposure and hence their CI could not be calculated. LLDPE, however, takes longer duration to reach the same level of degradation in terms of CI when exposed to either type of degrading environment. FTIR study further confirms our previous conclusion that the ability of manganese stearate pro-oxidant to initiate degradation in different grades of polyethylene follows the order LDPE > LDPE-LLDPE blends >LLDPE. Similar increase in CI is observed in films when exposed to xenon arc weathering, the effect being more pronounced in this case due to the combined effect of temperature as well as irradiation (550 W/m^2). The absorption due to other groups generated as a result of degradation i.e. hydroxyl and vinyl have been reported to follow the same trend as that of carbonyl, and hence are not being presented here.

The elemental analysis of films before and after degradation, was performed to quantify the oxygen content in the polymeric matrix, which is present in the form of aldehydes, esters, carboxylic acids etc. The carbon and hydrogen concentrations in all the polyethylene samples was 85.7% ± 0.2% and 14.3% ± 0.1% respectively, the oxygen concentrations being negligible. After 200 h of xenon exposure, the oxygen content in neat LLDPE and LDPE samples increased to 1.18% and 1.30% respectively, while that of samples containing manganese stearate increased to much higher extent. For LLMS75, LMS50, LMS75, and LMS100, the oxygen concentration increased to 4.67%, 5.02, 5.3, and 5.9% respectively after 50 h of xenon lamp exposure, which further confirm the development of oxygen containing functional groups on the polymer.

Melt flow index

The abiotic degradation in the presence of pro-oxidant is expected to cause chain scission in the

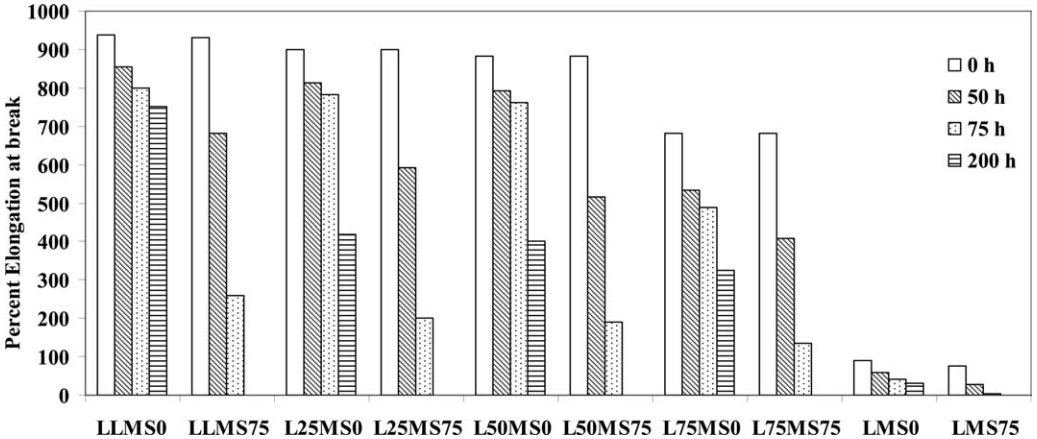

Figure 4 Variation in percent elongation as a function of xenon arc exposure.

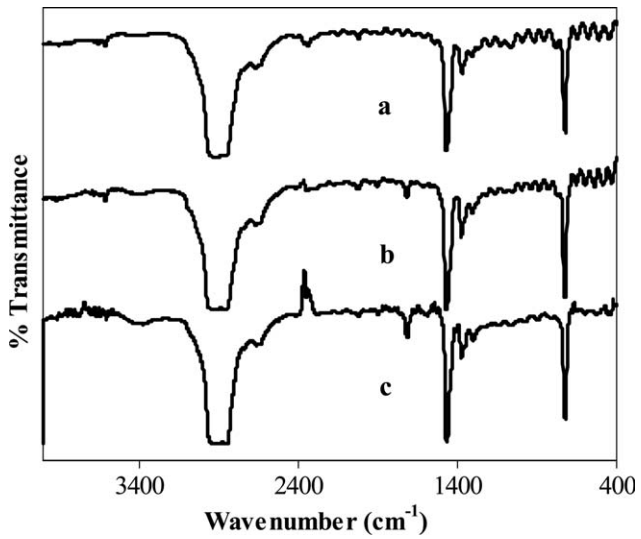

Figure 5 FTIR spectra of L75MS0 (a) 0 h, (b) 200 h of air oven aging, (c) 200 h of xenon arc exposure.

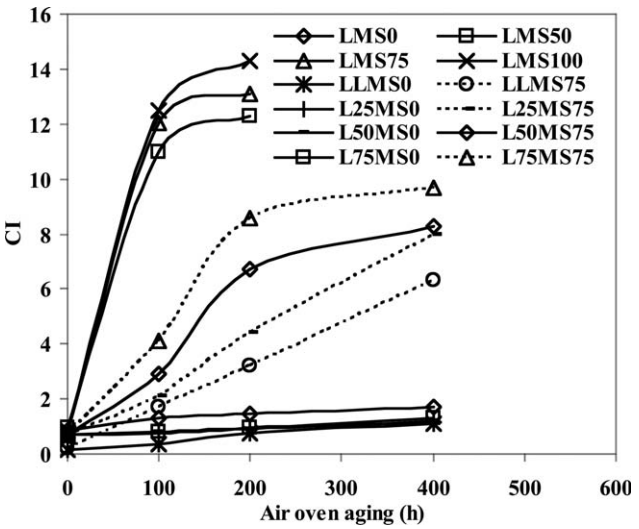

Figure 7 Increase in carbonyl index as a function of air–oven aging.

polymer resulting in the lowering of molecular weight. The decrease in the molecular weight is confirmed by investigating the increase in the MFI values, which was determined at 190°C under a dead weight of 2.16 kg (Table II). Because of the large amounts of sample required for the analysis, this test was performed for selected sampling intervals only. LDPE samples containing pro-oxidant, degraded to such an extent that it was practically impossible to determine the MFI after ~ 75 h of xenon arc lamp exposure and thermal exposure. The degradation in LLDPE and blends containing pro-oxidants was relatively lesser and required a minimum of 400 h of air oven aging and 200 h of xenon exposure to reach the stage when it started flowing under the MFI testing conditions.

Thermal properties

Figure 9 depicts the TGA traces of a representative sample (L25MS75) before and after xenon arc exposure of 200 h. It can be seen that the xenon arc irradiated sample of L25MS75 starts decomposing at much lower temperature after the exposure i.e. there is a substantial decrease in the initial decomposition temperature (IDT), from 350°C to 200°C. In our previous article, we have reported the formation of organic extractable products formed as a result of pro-oxidant initiated photo-oxidative degradation of LDPE, as identified by GC-MS.[9] These compounds include oxygenated molecules like alcohols, ketones, along with

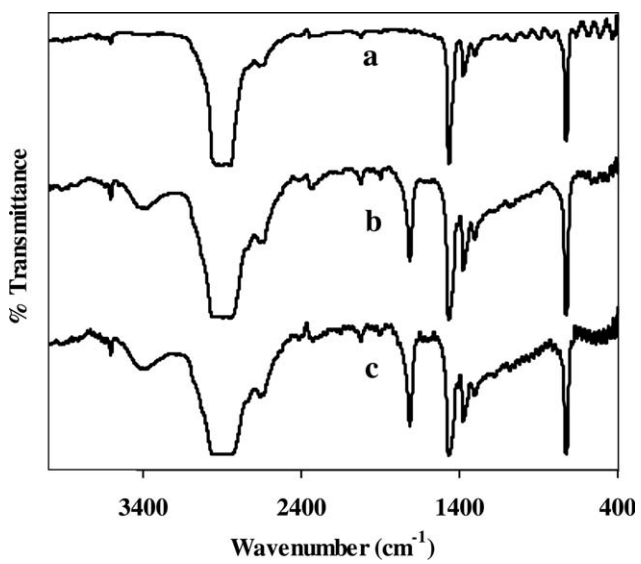

Figure 6 FTIR spectra of L75MS75 (a) 0 h (b) 200 h of air oven aging (c) 200 h of xenon arc exposure.

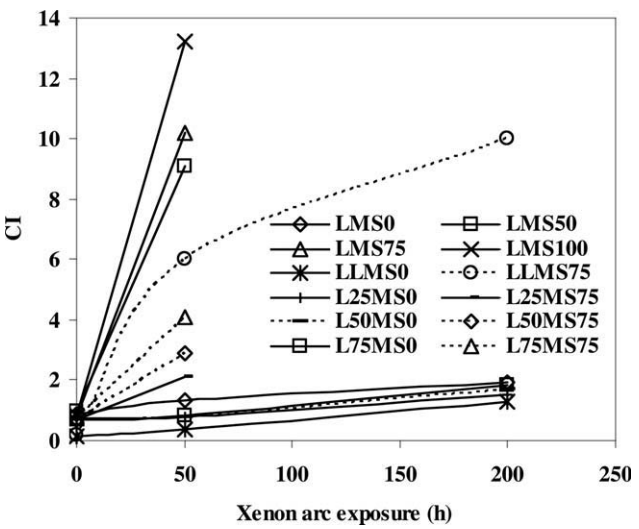

Figure 8 Increase in carbonyl index as a function of xenon arc exposure.

TABLE II
Effect of Accelerated Aging on the MFI of Formulations

	Melt flow index (g/10 min)			
	Xenon arc exposure (h)		Thermal exposure (h)	
Sample	0	200	200	400
LMS0	3.6	5.1	4.0	4.5
LMS50	3.6	[a]	[a]	[a]
LMS75	3.7	[a]	[a]	[a]
LMS100	3.7	[a]	[a]	[a]
LLMS0	0.9	2.1	1.0	1.2
LLMS75	0.9	[a]	9.1	[a]
L25MS0	1.4	4.0	2.1	2.3
L25MS75	1.4	[a]	10.2	[a]
L50MS0	2	4.2	2.9	3,2
L50MS75	2	[a]	11.2	[a]
L75MS0	2.8	4.3	3.8	3.9
L75MS75	2.8	[a]	13.3	[a]

[a] MFI could not be determined as the sample flowed under test conditions.

alkane and alkene hydrocarbons, all having lower decomposition temperatures. The presence of these degradation products can be used to account for the decrease in the observed IDT of the polymer.

However, no change in the melting point is observed as a result of degradation process. Thermal analysis also revealed that during the heating scans, LLDPE exhibited higher melting point (~ 120°C), as compared to LDPE (~ 110°C). However, during the cooling step, both LLDPE and LDPE develop crystallinity around the same crystallization temperature (~ 101°C). As a result of degradation, a broadening of the melting endotherm (during the heating scan) is observed, which amounts to increased DSC crystallinity. The DSC crystallinity of the samples as a function of exposure time has been presented in Table III. Actually the phenomenon of melting is associated only with the crystalline regions of the polymer, which remains practically unaffected during degradation, as it is restricted to the amorphous regions only. The broadening of the melting endotherm can also partially attributed to the changes in the crystalline sizes, molecular weight differences, which result from chain breaking and secondary crystallization.

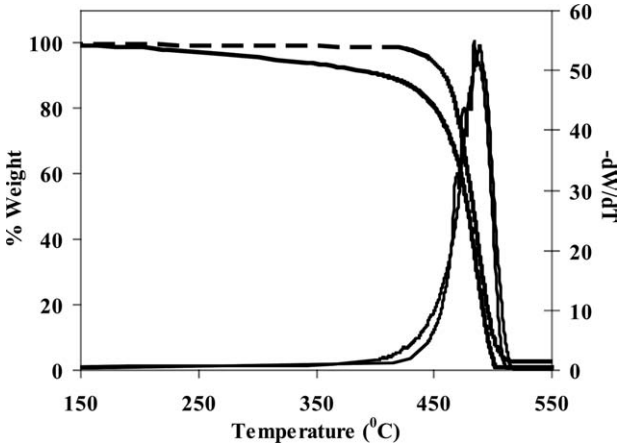

Figure 9 TG/DTG traces of L25MS75 (a) 0 h (b) 200 h of xenon arc exposure.

Surface morphological studies

Changes in the surface morphology was investigated using scanning electron microscopy. Figures 10 and 11 show the SEM of LLMS0 and LLMS75 before and after 200 h xenon arc exposure at a magnification of × 2000. Initially, films had a smooth surface, however they developed some cracks and grooves after the exposure. The extent of damage was much more pronounced in the samples containing pro-oxidant [Fig. 11(a,b)] as compared to neat LLDPE. As is evident, the progressive deepening of the craters/grooves result in the formation of defects/or weaker points which in turn affect the other properties also.

Kinetics of degradation

The thermogravimetric (TG) and derivative thermogravimetric (DTG) traces of LMS75 performed in nitrogen atmosphere at three different heating rates are presented in Figure 12. As expected, with an increase in the heating rate, there is a systematic shift in the TGA curves, and this has been used to evaluate the kinetic parameters using the Flynn-Wall-Ozawa method. This technique has previously been used to quantify the effect of another pro-

TABLE III
ΔH_f, ΔH_c and Percent Crystallinity of Films Before and After Xenon Arc Exposure

Sample designation	ΔH_f(J/g)		% Crystallinity		ΔH_c(J/g)	
	0 h	50 h	0 h	50 h	0 h	50 h
LMS0	128	141	44.9	49.5	−130	−146
LMS75	127	170	44.6	59.6	−133	−180
L50MS0	127	136	44.6	47.7	−136	−146
L50MS75	128	153	44.9	53.7	−137	−157
LLMS0	128	131	44.9	46.0	−140	−142
LLMS75	128	140	44.9	49.1	−143	−148

ΔH_f, heat of fusion; ΔH_c, heat of crystallization.

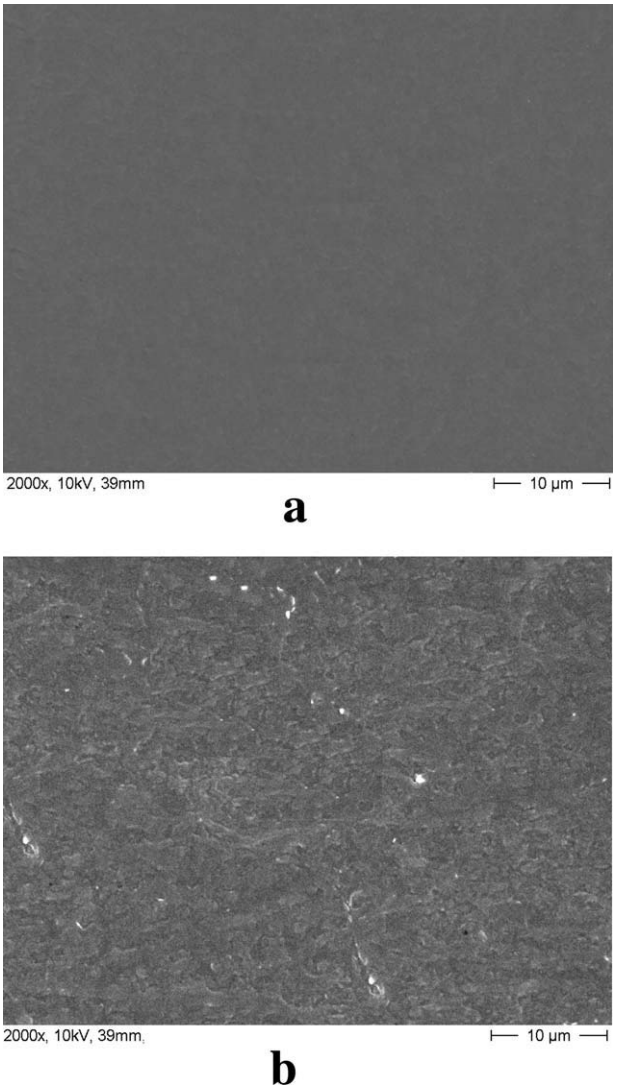

Figure 10 SEM of LLMS0 (a) initially (b) after 200 h of xenon arc exposure.

oxidant, cobalt stearate, on the theoretical lifetime of LDPE.[21]

Kinetic evaluations by Flynn-Wall-Ozawa method

The most common approach to determine the apparent kinetic parameters is first to measure the weight loss behavior during the material decomposition and then to employ the Arrhenius equation eq. (1) to fit this data.

$$\frac{d\alpha}{dt} = Ae^{\frac{-E_a}{RT}}(1-\alpha)^n \tag{1}$$

where A is the frequency factor, n is the reaction order, E_a is the apparent kinetic energy of the degradation reaction, R is the gas constant, α is the conversion and T is the absolute temperature. In thermogravimetric analysis, the conversion rate of a reaction is defined as the ratio of actual mass loss to the total mass loss corresponding to the degradation process.

$$\alpha = \frac{M_0 - M}{M_0 - M_f} \tag{2}$$

where M, M_0, and M_f are the actual, initial and final mass of the sample respectively. Ozawa, Flynn and Wall[22,23] derived a method for the determination of activation energy based on the equation:

$$\log\beta \cong 0.457\left(\frac{-E_a}{RT}\right) + \left[\log\left(\frac{AE_a}{R}\right) - \log F(\alpha) - 2.315\right] \tag{3}$$

where β is the heating rate. Thus, at the same conversion, the activation energy, E_a is obtained from the plot of log β against $1/T$.

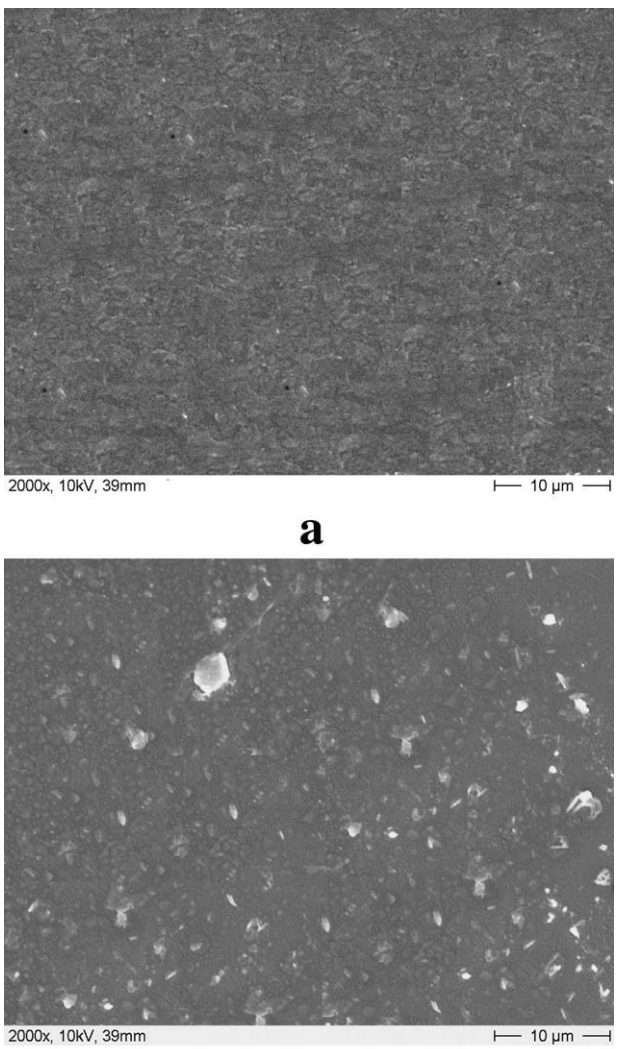

Figure 11 SEM of LLMS75 (a) initially (b) after 200 h of xenon arc exposure.

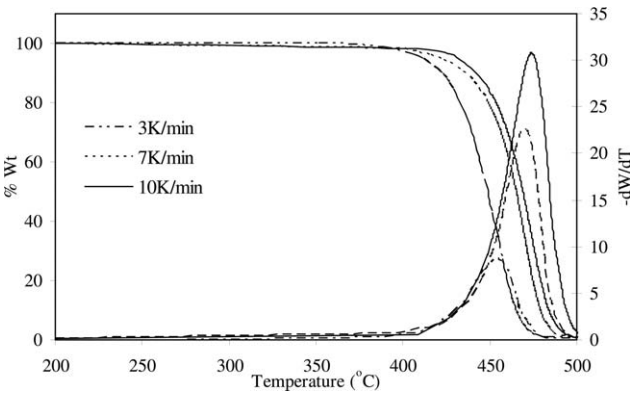

Figure 12 TG/ DTG traces of LMS0 at different heating rates under nitrogen.

Degradation kinetics in nitrogen

Based on eq. (3), the isoconversional graph between logarithm of heating rate (log β) and $1/T$ for different values of percentage conversion for samples were plotted and found to be almost parallel straight lines in nitrogen atmosphere. For both LDPE and LLDPE, the activation energy was found to be increase from 200 kJ/mol at lower degrees of conversion to ~ 280 kJ/mol at higher conversions. As has been reported by Peterson et al.,[24] the observed variation in the activation energy can be attributed to the degradation kinetics being governed by different processes at the initial and final stages, the lower value of the activation energy being associated with the initial process that occur at the weak links. Linear low-density polyethylene is a branched polymer containing olefinic branches, which can act as weak links. As these weak links are consumed, the limiting step of degradation shifts towards the degradation initiated by random scission, which requires higher energy. The activation energy "E_a" as well as frequency factor "A" were found to decrease significantly with increase in the concentration of manganese stearate. For LMS100, the E_a was found to be approximately 110–190 kJ/mol. This indicates that manganese stearate is capable of catalyzing the degradation process in polyethylene by providing an alternative route for degradation.

Lifetime predictions

The apparent kinetic parameters calculated from this study have been used to arrive at the theoretical lifetimes of the LLDPE formulations. The estimated lifetime of a polymer to failure has been defined as the time when the mass loss reaches 5 wt %, i.e. $\alpha = 0.05$.[25,26] The lifetime has been estimated by:

$$t_f = \frac{0.0513}{A} \exp \frac{E_a}{RT} \quad (n = 1)$$

Using the kinetic data and above equation, the estimated values of lifetime in nitrogen atmosphere at a mass loss of 5% at various temperatures are presented in Table IV. The theoretically calculated lifetime in nitrogen at 25°C decreased from 1.3×10^{19} min for LLDPE to 1.3×10^{10} min as the concentration of manganese stearate increased to 0.75% w/w. It can be seen that the lifetime is strongly dependant on the service temperature and decreased dramatically as the temperature increased from 25 to 200°C.

It should be noted here that the kinetics of the degradation process depend strongly on the chain mobility, which further depend on the physical state of the polymer. The chain mobility is much higher in the molten state than in the solid state thereby making the predictions relatively inaccurate at temperatures lower than melting point. Nonetheless, these studies confirm the degradative nature of manganese stearate on the degradation of LLDPE.

CONCLUSIONS

The present investigation reveals that introduction of trace quantities of manganese stearate into LDPE, LLDPE and their blends was capable of initiating rapid degradation of the polymeric chain when exposed to xenon arc weathering or air-oven aging. LDPE was found to more susceptible to degradation than LLDPE, because of the presence of large number of butyl branches, which act as weak linkages, and provide a site for generation of tertiary radicals. LLDPE on the other hand, being a copolymer of ethylene with olefins, like butene and hexane, has relatively lesser number of tertiary sites, thereby resisting degradation. The effect of xenon arc weathering on mechanical properties, increase in CI, crystallinity and MFI was found to be more pronounced than air oven aging at 70°C. The theoretical lifetimes of the polymers, as calculated by the Flynn-Wall-Ozawa technique, was found to decrease dramatically with increase in service temperature and the decrease

TABLE IV
Dependence of Lifetime on Service Temperature (Nitrogen Atmosphere)

	Lifetime (minutes)					
Sample	25°C	75°C	100°C	125°C	150°C	200°C
LLMS0	1.3×10^{19}	2.1×10^{16}	8.8×10^{13}	7.7×10^{11}	3.1×10^{8}	6.6×10^{5}
LLMS75	1.3×10^{10}	4.5×10^{8}	2.4×10^{7}	1.9×10^{6}	3.0×10^{4}	1.1×10^{3}

was more pronounced in the presence of manganese stearate pro-oxidant.

The authors thank J. C. Kapoor, Director, Centre for Fire, Explosive and Environment Safety, Delhi, India, for his keen interest and providing support to the study. They also thank Dr. R. Raman and Dr. Ashok Kapoor, SSPL, DRDO for FTIR and SEM analysis respectively.

References

1. Koutny, M.; Lemaire, J.; Delort, A.-M. Chemosphere 2006, 64, 1243.
2. Chiellini, E.; Corti, A.; Swift, G. Polym Degrad Stab 2003, 81, 341.
3. Chiellini, E.; Corti, A.; D'antone, S.; Baciu, R. Polym Degrad Stab 2006, 91, 2739.
4. Rabek, J. V. Polymer Photodegradation; Chapman and Hall: London, 1995.
5. Amin, M. U.; Scott, G. Eur Polym J 1974, 10, 1019.
6. David, C.; Trojan, M.; Daro, A.; Demarteau, W. Polym Degrad Stab 1992, 37, 233.
7. Roy, P. K.; Surekha, P.; Rajagopal, C.; Raman, R.; Choudhary, V. J Appl Polym Sci 2006, 99, 236.
8. Roy, P. K.; Surekha, P.; Rajagopal, C.; Chatterjee, S. N.; Choudhary, V. Polym Degrad Stab 2005, 90, 577.
9. Roy, P. K.; Titus, S.; Surekha, P.; Tulsi, E.; Deshmukh, C.; Rajagopal, C. Polym Degrad Stab 2008, 93, 1917.
10. Roy, P. K.; Surekha, P.; Rajagopal, C.; Choudhary, V. J Appl Polym Sci 2008, 108, 2726.
11. Khabbaz, F.; Albertsson, A. C. J Appl Polym Sci 2001, 79, 2309.
12. Grant, M. H., Ed. Encyclopedia of Chemical Technology; Wiley: New York, 1991; Vol. 8.
13. Collins, E. A.; Bares, J.; Billmeyer, F. W. Experiments in Polymer Science; Wiley-Interscience: New York, 1973; p 305.
14. Sharma, N.; Chang, L. P.; Chu, Y. L.; Ismail, H.; Ishiaku, U. S.; Ishak, Z. A. Polym Degrad Stab 2001, 71, 381.
15. Gulmine, J. V.; Janissek, P. R.; Heise, H. M.; Akcelrud, L. Polym Degrad Stab 2003, 79, 385.
16. Seeba, M.; Servens, C.; Pouyet, J. J Appl Polym Sci 1992, 45, 1049.
17. Osawa, Z.; Kurisu, N.; Nagashima, K.; Nankano, K. J Appl Polym Sci 1979, 23, 3583.
18. Osawa, Z. Polym Degrad Stab 1988, 20, 203.
19. Khabbaz, F.; Albertsson, A. C.; Karlson, S. Polym Degrad Stab 1998, 61, 329.
20. Lin, Y. J Appl Polym Sci 1997, 63, 811.
21. Roy, P. K.; Surekha, P.; Rajagopal, C.; Choudhary, V. Exp Polym Lett 2007, 1, 208.
22. Ozawa, T. Thermochim Acta 1986, 100, 109.
23. Flynn, J. H.; Wall, L. A. J Polym Sci Part B: Polym Lett 1966, 4, 323.
24. Peterson, J. D.; Vyazovkin, S.; Wight, C. A. Macromol Chem Phys 2001, 202, 775.
25. Li, X. G.; Huang, M. R. Polym Degrad Stab 1999, 64, 81.
26. Huang, M. R.; Li, X. G. J Appl Polym Sci 1998, 68, 293.